Available online at www.sciencedirect.com
SCIENCE DIRECT®
Journal of Magnetism and Magnetic Materials 272–276 (2004) 1631–1636
Journal of magnetism and magnetic materials
www.elsevier.com/locate/jmmm

Spin configurations and classification of switching processes in ferromagnetic rings down to sub-100 nm dimensions

M. Kläui[a], C.A.F. Vaz[a], T.L. Monchesky[b], J. Unguris[b], E. Bauer[c], S. Cherifi[d], S. Heun[d], A. Locatelli[d], L.J. Heyderman[e], Z. Cui[f], J.A.C. Bland[a,*]

[a] *Cavendish Laboratory, University of Cambridge, Madingley Road, Cambridge CB3 0HE, UK*
[b] *National Institute of Standards and Technology, Gaithersburg, MD 20899, USA*
[c] *Department of Physics and Astronomy, Arizona State University, Tempe, AZ 85287-1404, USA*
[d] *Sincrotrone Trieste, 34012 Basovizza, Trieste, Italy*
[e] *Laboratory for Micro- and Nanotechnology, Paul Scherrer Institut, Villigen PSI CH-5232, Switzerland*
[f] *Rutherford Appleton Laboratory, Chilton Didcot OX11 0QX, UK*

Received 17 January 2003; received in revised form 8 July 2003

Abstract

The magnetic states and switching processes are investigated in Co and NiFe rings with lateral dimensions from the micrometer range down to sub-100 nm. Using non-intrusive imaging techniques we have directly observed the nanoscopic details of the magnetization configurations of epitaxial and polycrystalline mesoscopic ring structures with <15 nm resolution. We have found head-to-head domain walls with different spin structures depending on ring width. Further, we can classify the geometry-dependent switching processes according to the number of transitions (single, double, triple) that a ring undergoes in a hysteresis cycle. In the case of triple switching we find a novel state with a complete vortex core present in the ring. It is found that the double switching can be retained in sub-100 nm rings by tailoring the material and thickness.

PACS: 75.60.Ej; 75.60.Ch; 75.70.Ak; 85.70.Kh

Keywords: Magnetic rings; Magnetic switching; Magnetic imaging; Micromagnetics

1. Introduction

Intensive research has been recently devoted to understanding and controlling the magnetic properties of small ferromagnetic elements. This is not only due to the fact that these structures allow for the investigation of fundamental physical properties [1] but they also have important applications such as in magnetic random access memory (MRAM) cells [2]. One key issue is to understand and control the magnetic switching precisely. To achieve this one needs firstly to have well defined and reproducible remanent states and secondly, the switching process itself must be simple and reproducible. A possible geometry that fulfills these criteria is the ring geometry, and in particular narrow ferromagnetic rings, which have recently become the focus of intense interest [3–10]. In all the ring geometries investigated so far, macroscopic measurements and micromagnetic simulations suggest the existence of two magnetic states [3,4,6,7]: the flux-closure vortex state and the 'onion' state, accessible reversibly from saturation and characterized by the presence of two opposite head-to-head walls. The details of the magnetization configurations in these states was primarily inferred from the comparison of macroscopic measurements

*Corresponding author. Tel.: +44-1223-337426; fax: +44-1223-350266.
E-mail address: jacbl@phys.cam.ac.uk, jacb1@cam.ac.uk (J.A.C. Bland).

0304-8853/$ - see front matter © 2004 Elsevier B.V. All rights reserved.
doi:10.1016/j.jmmm.2003.12.1365

(e.g. MOKE) with subsequent micromagnetic simulations [3,11,12]. However, since it is the microscopic spin configuration of the magnetic states that governs the macroscopic magnetic properties and switching, non-intrusive imaging of the microscopic details of the magnetization including the exact spin structure of the head-to-head domain walls at the nanometer scale is needed in order to understand and control the switching processes [3,11,12]. Furthermore, the geometry and the magnetocrystalline anisotropy are predicted to determine the microscopic spin structure of the magnetic states [11,13], for which direct experimental evidence so far is unavailable. In this paper we review the result of our recent work using non-intrusive imaging techniques based on photoemission electron microscopy (PEEM), and for higher resolution, scanning electron microscopy with polarization analysis (SEMPA) to directly observe the different magnetization configurations present in polycrystalline and epitaxial ring geometries, including details of the different types of head-to-head domain walls. Furthermore, the geometry and material dependence of the switching is comprehensively reviewed using both magneto-optical Kerr effect (MOKE) and micromagnetic simulations for rings down to sub-100 nm lateral dimensions. We find additional novel states and transitions that allow us to classify the observed switching behaviour of all mesoscopic rings into three categories.

Two methods were used to fabricate rings with lateral dimensions from the micrometer scale to sub-100 nm diameters: lift-off of polycrystalline Co and Permalloy (NiFe) films grown on naturally oxidized Si (0 0 1) [5,14] and epitaxial growth of Co on prepatterned Si (0 0 1)-H substrates [3]. For the latter method, the epitaxial rings were obtained by depositing a trilayer Cu(100)/FCC Co(100)/Cu(100) capped with 4 nm Au on a Si (100) prepatterned wafer in a UHV MBE system (base pressure 3×10^{-10} mbar) [3]. An advantage of structures on pre-patterned substrates is that, in contrast to conventional methods, no patterning processes that might alter the properties are applied to the magnetic material. A 4 nm Au capping layer was grown under non-normal incidence and rotation, which gives lateral protection from oxidation. The lift-off rings were fabricated by means of a PMMA mask that was patterned by e-beam [5,14,15]. This was followed by the MBE deposition in UHV and lift-off of polycrystalline Co or permalloy layers with 4 nm of Au to prevent oxidation.

2. Magnetostatic states in rings

To image the magnetization configurations we chose PEEM and SEMPA, which are non-intrusive techniques in contrast to imaging techniques such as magnetic force microscopy (MFM) (as shown in MFM imaging of octagonal structures, MFM can influence and even switch the magnetic configurations [6]). Furthermore, unlike MFM, the non-intrusive techniques used here allow us to image even magnetic states with no stray field such as the vortex state. PEEM was carried out at the synchrotron ELETTRA in Trieste [16]. In X-ray magnetic circular dichroism PEEM (XMCDPEEM) the secondary electrons created in the photoexcitation of 2p electrons into states just above the Fermi level are used for imaging. With circular polarized light (polarization $\boldsymbol{\sigma}$) the excitation probability and, therefore, also the secondary yield depends upon the dot product of $\boldsymbol{\sigma}$ and the magnetic spin moment $\mathbf{m}$, which is then visible as contrast in the images [16]. To achieve a higher resolution than that possible with MFM or PEEM, scanning electron microscopy with polarization analysis (SEMPA) was performed at the National Institute of Standards and Technology (NIST) [17]. In this technique, the scanning electron microscope geometry is extended to include spin polarization sensitive detection of the scattered electrons. In this study SEMPA was used to measure the in-plane magnetization direction. To investigate the switching behaviour, MOKE was used to measure hysteresis loops as described in Ref. [3]. Simulations were computed by solving the micromagnetic equilibrium equation for each applied field on a square mesh, with a 4 nm cell size. A conjugate gradient solver and the OOMMF package[1] were used for the energy minimization and yielded similar results. The intrinsic parameters used for Co are: $M_s = 1424 \times 10^3$ A/m, $A = 33 \times 10^{-12}$ J/m and $K_1 = 6.5 \times 10^4$ J/m^3 for epitaxial rings while $K_1 = 0$ in the polycrystalline case. For permalloy we used: $M_s = 800 \times 10^3$ A/m and $A = 13 \times 10^{-12}$ J/m.

As shown in Ref. [3], we can use an appropriate minor loop field path to obtain rings in the onion state or in the vortex state at remanence. Since we measure an array of rings with a switching field distribution we can switch some of the rings into the onion state while some will remain in the vortex state by following the field path indicated by the red arrows in the hysteresis loop in Fig. 1(a), where the field is relaxed to zero from the middle of the switching field distribution of the vortex to the onion transition [3]. A low-resolution PEEM image of four rings (outer diameter $D = 1200$ nm, inner diameter $d = 900$ nm and thickness $t = 15$ nm polycrystalline Co), taken after relaxation of the field to remanence, is shown in Fig. 1(b). As expected some rings are still in the vortex state (two rings have a counter-clockwise and one ring has a clockwise circulation direction) while one ring has already switched into the onion state. While it is easy to confirm the vortex and onion states with PEEM, the

[1] The public domain package is available at gams.nist.gov/oommf.

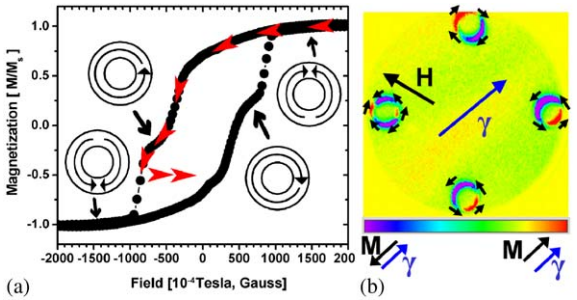

Fig. 1. (a) Hysteresis loop measured on an array of rings (outer diameter $D = 1200$ nm, inner diameter $d = 900$ nm and thickness $t = 15$ nm polycrystalline Co). The magnetization configurations of the onion and the vortex states are shown schematically. Red arrows indicate the field path used to obtain the rings in the states imaged with PEEM in (b). (b) PEEM image of four polycrystalline Co rings. The top ring is in the clockwise vortex state, the bottom and right rings are in the counter-clockwise vortex state and the left ring is in the onion state pointing along the direction of the applied field H. The field of view is ≈ 10 μm across and the blue arrow points in the direction of the photon beam. The colour scale indicates the direction of the magnetization with reference to the direction of the incoming photon beam (magnetization parallel to the incoming photon beam (red) to anti-parallel (purple)). For colour, please see on-line version.

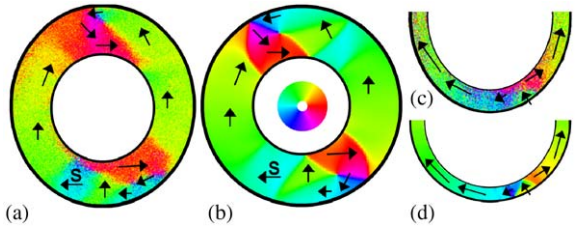

Fig. 2. Micromagnetic calculations and SEMPA images of the onion state in a wide ($D = 1700$ nm, $d = 900$ nm) and a narrow ($D = 1700$ nm, $d = 1200$ nm) epitaxial 34 nm FCC Co ring. (a) SEMPA image of the wide ring. The vortex walls and the magnetocrystalline anisotropy induced domain structure (marked with S) is visible. (b) Micromagnetic simulation of the wide ring. In addition to the vortex head-to-head domain wall, the domain structure is visible (marked with S). The colour code indicating the direction of the magnetization is shown in the on-line version of this figure. (c) SEMPA image of the narrow ring (only half the ring is shown). No domain structure is seen as the local shape anisotropy dominates over the magnetocrystalline anisotropy. A transverse head-to-head domain wall is present. (d) Micromagnetic simulation of the narrow ring exhibiting the transverse domain wall.

maximum resolution achieved (30 nm) is not sufficient to resolve the details of the exact magnetization configuration such as the structure of the head to head domain walls in the onion state.

To obtain more detailed, higher resolution images we use SEMPA. Higher resolution is essential since micromagnetic simulations predict different types of head to head domain walls [11], and since it is the type of domain wall that characterizes the onion state and is very important for the switching behaviour investigated in Ref. [12,13] and for the nucleation-free onion to vortex transition [3]. For epitaxial samples (e.g. FCC cobalt), micromagnetic simulations predict that, in addition to the head to head domain walls that are also present in the onion state of polycrystalline rings, epitaxial samples should show additional domain-like features due to the cubic anisotropy. Furthermore, epitaxial samples of different geometries also allow the study of the interplay between the magnetocrystalline anisotropy and the local shape anisotropy that is due to the dipolar interactions in the particular geometry. A SEMPA image for a wide epitaxial ring ($D = 1700$ nm, $d = 900$ nm, $t = 34$ nm FCC Co) is shown in Fig. 2(a). In this wide ring the head-to-head wall is a vortex wall, since this minimizes the stray field without significantly increasing the exchange energy term as theoretically predicted [11]. The micromagnetic simulation in Fig. 2(b) shows remarkable agreement, although the exact position of the head-to-head domain wall in the experiment is determined by local defects (the highly energetic vortex core is pinned at non-magnetic defects). In addition to the head-to-head walls, a domain structure is visible in the SEMPA image and in the simulation, demonstrating the influence of the magnetocrystalline anisotropy for this wide ring geometry.

In narrow rings any deviation of the magnetization from parallel to the ring edge will create dipole stray fields. Therefore, the magnetization closely follows the shape (local shape anisotropy) and aligns with the circumference. In this case no domain features are expected since the strong local shape anisotropy supersedes the magnetocrystalline anisotropy. This can be seen in the SEMPA image in Fig. 2(c) and in the micromagnetic simulation in Fig. 2(d) of a narrow ring ($D = 1700$ nm, $d = 1200$ nm, $t = 34$ nm FCC Co). Furthermore in this narrow ring a transverse head-to-head domain wall is present since a vortex wall would have to be compressed into the narrow ring resulting in a prohibitively high exchange energy. The energetics of the different domain wall types is analysed further in Ref. [11] and the different kinds of domain walls observed here are in good agreement with Ref. [11].

3. Magnetodynamic switching in rings

While the geometry dependence of the remanent magnetic states can be studied with SEMPA, it is difficult to image while applying magnetic fields. To study the magnetic states and transitions, which develop when a field is applied, we carried out MOKE

measurements on arrays of rings. In the limited range of geometries and materials that have been studied previously [3,4,6] the double switching process discussed above was reported. Here we have varied the film thickness and ring width over a very wide range (film thickness FCC Co 5–34 nm, polycrystalline Co 2–34 nm and polycrystalline permalloy 2–45 nm, ring width 5–90% of the outer diameter D, 90 nm $< D <$ 2000 nm). D is kept <2 μm for mesoscopic rings to prevent the occurrence of complicated and defect dominated multi-domain states and the minimum diameter is set by limitations in the fabrication process as detailed in Ref. [18]. From our micromagnetic simulations it can be seen that as the lateral size of the rings is reduced, the vortex state becomes more and more unfavourable due to the increasing curvature of the ring, which results in an increased exchange energy. Since it is the stray field-free vortex state that has been suggested for applications in data storage [2], it is of paramount importance to establish whether the double switching process where the vortex state is attained exists in the smallest rings, and how the switching fields develop when the lateral dimensions are reduced. To check this, we have thus used a soft magnetic material (permalloy) for the small rings. We find that even for the smallest rings we can obtain a double switching if we deposit a sufficiently thick film, e.g. 10 nm of permalloy [18]. In Fig. 3 a hysteresis loop of an array of rings is presented ($D = 110$ nm, $d = 60$ nm and $t = 10$ nm polycrystalline permalloy), which exhibits a double switching. Fig. 3(e) shows the onion to vortex (black squares) and vortex to reverse onion (black discs) switching fields as a function of outer diameter for rings with a constant ring width (25 nm) and thickness (10 nm permalloy). The high switching field of the vortex to reverse onion transition can be explained by the fact that the ring width is narrow as also observed in Ref. [15]. This vortex to reverse onion switching field is only weakly dependent on the outer diameter, while the onion to vortex switching field increases significantly with increasing outer diameter. To explain this behaviour we have to take into account that the process for this transition is a domain wall depinning and propagation process [3]. The effective field working to displace the wall is the field component that is parallel to the direction of the domain wall movement, hence the component parallel to the perimeter. If the domain wall positions are perfectly aligned with the field direction, this component is zero (field and domain wall positions are antiparallel). Due to local imperfection the domain wall will be always misaligned a few nm with the field direction and in the case of a small outer diameter this displacement will lead to a large field component parallel to the displacement direction, whereas in a ring with a large outer diameter this displacement will mean that the working field component is only slightly increased from zero.

In addition to the previously found double switching process (Figs. 1(a), 3, [3,4]), depending on the geometry we find novel types of hysteresis behaviour: the reversal can occur with a single transition as seen in Fig. 4(a) or with triple switching as seen in Fig. 4(b).

To elucidate these different behaviours we consider the transitions that are available for each magnetic state. After relaxing the field from saturation a ring develops the onion state with a wall structure determined by the geometry (see Fig. 2(a)–(d)). Additional simulations show that then there are two competing switching processes when a reverse field is applied: (i) for rings

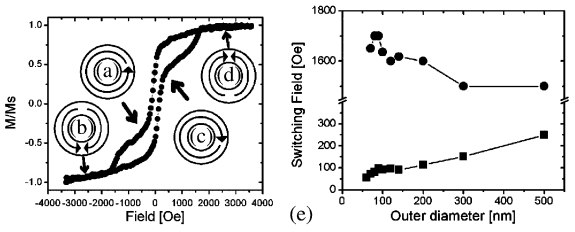

Fig. 3. MOKE measurement on an array of rings ($D = 110$ nm, $d = 60$ nm and $t = 10$ nm polycrystalline permalloy) showing double switching and schematic representation of the magnetic states (inset (a)–(d)). The graph (e) shows the switching fields (extracted as explained in Ref. [15]) of the onion to vortex transition (black squares) increasing with outer diameter, whereas the vortex to reverse onion switching field (black discs) is only weakly dependent on the outer diameter for rings with a constant width and thickness ($(D - d)/2 = 25$ nm, $t =$ 10 nm Py).

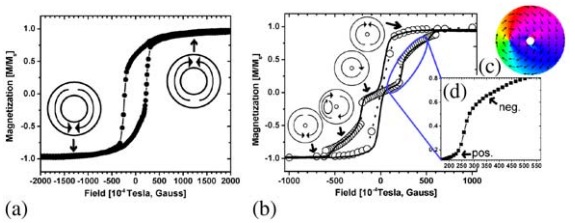

Fig. 4. MOKE loops of an array of rings. (a) Hysteresis loop showing single switching in thin film rings ($D = 1700$ nm, $d =$ 1250 nm, $t = 4$ nm polycrystalline Co) with the magnetization configurations of the onion states shown schematically. (b) Triple switching in very wide rings with thick films ($D = 1700$ nm, $d = 300$ nm, $t = 32$ nm polycrystalline Co; experimental data: black line, micromagnetic simulation: empty circles). The magnetization configurations are shown schematically (from top to bottom: onion, vortex, vortexcore and opposite onion state). (c) Micromagnetic simulation of the magnetization configuration in the vortexcore state (colour code as in Fig. 2). (d) Enlargement of the experimental data in the interesting field region showing the difference in curvature when the field is applied to the ring in the vortex state (indicated with pos.) and in the vortexcore state (indicated with neg.)

made of a thick magnetic film, domain wall depinning followed by propagation leads to the double switching process as seen in Fig. 1(a) and explained in Refs. [3,19]; (ii) in rings with a thin film a reverse domain can be nucleated somewhere at the edge of the ring (where the torque on the spins is large, not necessarily related to the position of the domain walls), which then grows and spreads over the whole ring until the opposite onion state is attained. This process is a nucleation–propagation process similar to that described in detail in [19] but in this case it leads to a single onion to (reverse-) onion switching characterized by a single jump in the M–H loop (Fig. 4(a)). This process is very unfavourable in thick film rings since the spins are strongly aligned with the edges. Any deviation from the perimeter would be energetically disadvantageous in this case due to the large dipolar stray field created, whereas in thin rings the necessary twisting of spins to nucleate a reverse domain can happen easily. Furthermore in very thin rings the onion state can be energetically favoured over the vortex state because of the lower exchange energy, which outweighs the small stray field energy of the onion state, so that as seen in Fig. 4(a) a very thin ring ($t = 4$ nm here) switches directly from the onion to the reverse onion state. To explain the triple switching observed for wide and very thick rings (e.g. the ring geometry for Fig. 4(b)), we have computed a hysteresis loop for such a ring. As seen in Fig. 4(b) the simulation reproduces the experimental loop well and the magnetization configurations found are shown schematically. Apart from the onion and vortex state, we observe a new state (schematic in Fig. 4(b) and micromagnetic simulation of the detailed magnetization configuration in Fig. 4(c)), which we term the 'vortexcore' state (since a complete vortex core is present). This state is not stable at remanence, where the ring reverts to the vortex state. This is because both states have zero stray field but the exchange energy is higher in the vortexcore state due to the presence of the vortex core. In an applied field on the other hand the gain in Zeeman energy in the vortexcore state makes it energetically favourable. As the vortexcore state has to be stabilized by an applied field, it could not be directly imaged with the techniques available, but we can compare the simulated and measured hysteresis loops shown in Fig. 4(b). The height of the jumps is well reproduced in the simulation. In addition a very sensitive measure for the type of magnetization configuration is the curvature of the loop when the field is applied. As predicted earlier [21] the curvature d^2M/dH^2 of the hysteresis loop is positive when a field is applied to a ring in the vortex state and negative if the ring is in a state where a vortex core is present, such as the vortexcore state. As seen in Fig. 4(b) and the enlargement of the interesting field region Fig. 4(d), the curvature after the first switching is positive, which means that the rings have switched from the onion state into the vortex state. After the second jump the curvature is negative, which means that the ring has switched from the vortex to the vortexcore state. This negative curvature is the same as that reported for the case of discs in the vortex state in an applied field [20,21]. The similarities in the curvature are due to the fact that physically the same process is occurring as the applied field is increased: the component of the magnetization parallel to the field direction grows and hence the vortex core is pushed outwards (in the case of Fig. 4(b) towards the left) until at the critical field it leaves the structure and the ring attains the onion state. It is now clear why the vortexcore state is only observed in wide and very thick rings: due to the exchange energy it is only possible to 'fit' a vortex core into rings above a certain width and only for large thicknesses the energy gain due to the absence of a stray field offsets the higher exchange energy of the vortexcore state.

In conclusion, we have presented the nanoscopic details of the magnetization configurations in mesoscopic rings, which show the influence of geometry and magnetocrystalline anisotropy particularly on the spin structure of the different types of head to head domain walls. The influence of the geometry on the switching processes is evident and three categories of switching behaviour are found. The double switching process is found in most rings, including rings with sub-100 nm outer diameters. In addition to this double switching process, thin rings show a single reversal mechanism, while very wide rings with a thick film exhibit triple switching and for these rings the novel vortexcore state is shown to occur.

Acknowledgements

The authors acknowledge support from the Gottlieb Daimler- and Karl Benz Foundation (M.K.), the Office of Naval Research (T.L.M. and J.U.) and the European ESPRIT network MASSDOTS (22464), the CMI project 'Magnetoelectronic devices' and DAAD.

References

[1] L.D. Landau, et al., Physik. Z. Sowjetunion 8 (1935) 153.
[2] J.-G. Zhu, et al., J. Appl. Phys. 87 (2000) 6668.
[3] J. Rothman, et al., Phys. Rev. Lett. 86 (2001) 1098.
[4] M. Kläui, et al., Appl. Phys. Lett. 78 (2001) 3268.
[5] M. Kläui, et al., Appl. Phys. Lett. 81 (2002) 108.
[6] S.P. Li, et al., Phys. Rev. Lett. 86 (2001) 1102.
[7] S. Kasai, et al., J. Magn. Magn. Mater. 239 (2002) 228.
[8] J. Bekaert, et al., Appl. Phys. Lett. 81 (2002) 3413.
[9] X. Zhu, et al., J. Appl. Phys. 93 (2003) 8540.
[10] M. Kläui, et al., Phys. Rev. Lett. 90 (2003) 97202.
[11] R.D., McMichael, et al., IEEE Trans. Magn. 33 (1997) 4167.

[12] L. Lopez-Diaz, et al., Physica B 306 (2001) 211.
[13] L. Lopez-Diaz, et al., J. Appl. Phys. 89 (2001) 7579.
[14] C. David, et al., Microelectron. Eng. 46 (1999) 219.
[15] Y.G. Yoo, et al., Appl. Phys. Lett. 82 (2003) 2470.
[16] A. Locatelli, et al., Surf. Rev. Lett. 9 (2002) 171.
[17] M.R. Scheinfein, et al., Rev. Sci. Instrum. 61 (1990) 2501.
[18] L.J. Heyderman, et al., J. Appl. Phys. 93 (2003) 10011.
[19] M. Kläui, et al., J. Magn. Magn. Mater. 240 (2002) 7.
[20] R.P. Cowburn, et al., Phys. Rev. Lett. 83 (1999) 1042.
[21] L. Lopez-Diaz, et al., IEEE Trans. Magn. 36 (2000) 3155.